JOURNAL OF MATERIALS SCIENCE **36** (2001) 5027–5030

Preparation and characterization of Ce-doped $BaTiO_3$ thin films by r.f. sputtering

M. CERNEA, I. MATEI, A. IUGA, C. LOGOFATU
National Institute for Physics and Technology of Materials, 76900, Bucharest
E-mail: mcernea@alpha1.infim.ro

Ce-doped $BaTiO_3$ thin films prepared on silicon-platinium by r.f. sputtering has been investigated. $BaTiO_3$ doped with 5.5 mol%CeO_2 thin film was deposited at 550°C substrate temperature in an Ar atmosfere. The crystal structure and shape were examined by X-ray diffraction and scanning electron microscopy with EDAX. Analysis by X-ray diffraction patterns show that the crystalline film with a cubic structure of $BaTiO_3$, was obtained. The surface morphology (roughness, the grain size and the droplet size) of the thin film surface was examined by atomic force microscopy (AFM). The grain size is about 160 nm, the droplet size is about 0.675 μm and the roughness is 36.88 nm. EDAX analysis established a composition of the film to be identical with that of the target ($BaTiO_3$ doped with 5.5 mol%CeO_2). The broad peak in the capacitance versus temperature curve at the Curie point indicate that the r.f. sputtered Ce-doped $BaTiO_3$ film is ferroelectric. The values of the capacitance of the thin film at 1 KHz were found to be 86 pF and the loss dielectric was $\tan\delta = 0.0875$. The film exibits a dielectric anomaly peak at 23°C showing ferroelectric to paraelectric phase transition.

1. Introduction

Barium titanate ($BaTiO_3$) is a ferroelectric material widely studied because of its many potential useful properties. There are numerous proposals for its application in electronic [1–4] and electro-optic devices [5–7] apart from its high permittivity phenomena, associated with the basic ferroelectric behaviour. Obtaining thin films of $BaTiO_3$ and doped $BaTiO_3$ with properties approaching those of bulk $BaTiO_3$ (and doped-$BaTiO_3$) would both contribute general insight into thin-physics and also have application in the microelectronic industries. Extensive work has been done using r.f. sputtering and other thin-film fabrication techniques [8–11]. Preparation of $BaTiO_3$ thin films by sputtering was intensely studied to find the influences of procesing parameters on the thin films quality [9, 12, 13]. Nagatomo *et al.* [9] reported the relationship between the substrate temperature and total gas pressure for the fabrication of $BaTiO_3$ films on platinium and fused quartz substrates by r.f. planar-magnetron sputtering. They obtained various structural films with no phase transition occuring. Another paper on the preparation of $BaTiO_3$ films by sputtering [13], described the dependence of amorphous, cubic and tetragonal phase transitions on the substrate and annealing temperatures.

In this paper, the preparation and characterization of thin films of CeO_2-doped $BaTiO_3$ are reported.

2. Experimental procedure

A SBR-1102E (ULVAC) r.f. sputtering system was used to make the Ce-doped $BaTiO_3$ thin film on silicon-platinium substrates. A chromel-alumel thermocouple was attached to control the temperature of the substrate. The powder for the target was prepared from $BaTiO_3$, CeO_2 and TiO_2. From barium chloride, titanium chloride and oxalic acid we precipitated $BaTiO(C_2O_4)_2 \cdot 4H_2O$ following the reaction [14]:

$$TiCl_4 + BaCl_2 + 2H_2C_2O_4 \rightarrow BaTiO(C_2O_4)_2 \cdot 4H_2O + 6HCl,$$

This process leads to a high-purity titanate with a Ba/Ti ratio near to 1.00 and very small grains of about 0.6 μm, by calcination up to 900°C [15–20]. We added CeO_2 and TiO_2 in molar ratio 1 : 1 to $BaTiO_3$. The concentration of the donor dopant CeO_2 was 5.5 mol%. The sputtering chamber was initially evacuated to a base pressure of 3×10^{-3} Pa, then argon gas, controlled with a separate flowmeter, was introduced into the sputtering chamber until a presure of 1 Pa. The substrate was clamped on a steel substrate holder at 550°C. The sputtering conditions are summarized in Table I.

Single-crystal silicon wafers doped with phosphorous (n-type) and cleaved parallel to the (100) plane were used as substrate material for a platinum thin film deposited by sputtering at 550°C. Before the Pt film deposition, the wafers were thoroughly cleaned and etched in an HF buffer solution to strip off the SiO_2 layer. To test the ferroelectric properties of Ce-modified $BaTiO_3$ film, a structure was formed from a Ti film as the lower electrode and a layer of silver. We used a Philips DRON 3 for X-ray diffraction and a SEM515 with EDAX, for the surface morphology analysis. Capacitance and dielectric loss were measured

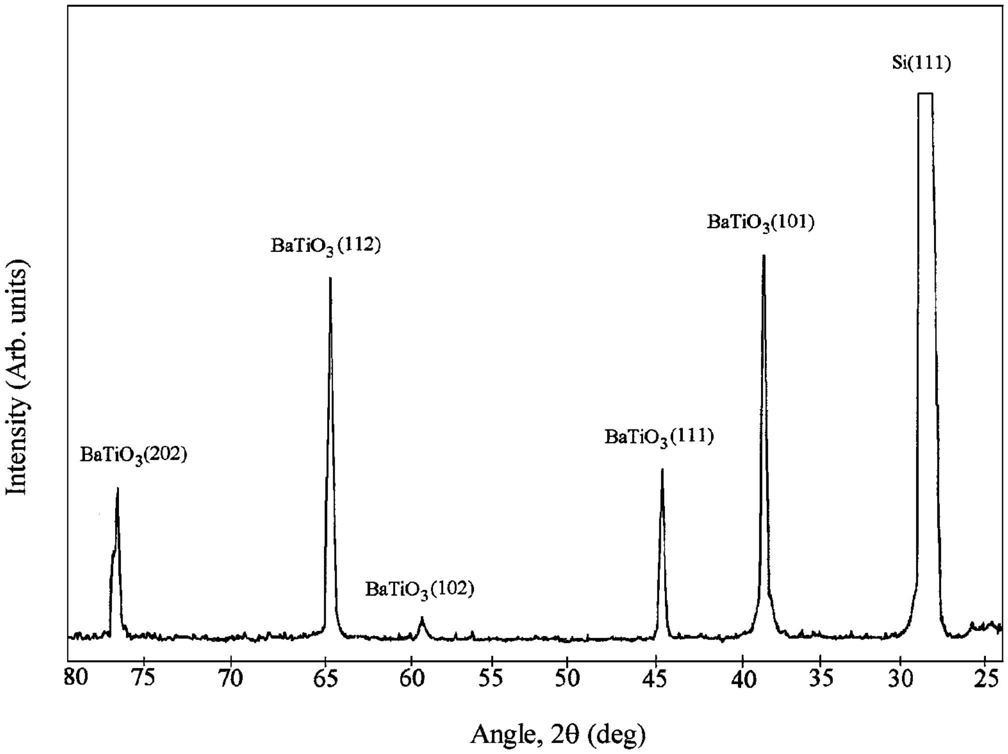

Figure 1 XRD patterns of $BaTiO_3$ doped with 5.5 mol%CeO_2 film.

TABLE I Summary of sputtering conditions

Target to substrate distance	30 mm
Sputtering gas	100
Vol%Ar	
Gas pressure	1 Pa
Substrate	Si-Pt
Substrate temperature	550°C
Deposition rate	2.5 nm/min
Thickness sputered film	900 nm

at 1 KHz characteristic frequency using a Hewlett-Packard Model 4194A impedance meter.

3. Results and discussion

The structure of Ce-doped $BaTiO_3$ film deposited on Si-Pt was studied by X-ray diffraction technique using Cu K_α radiation at room temperature. The film deposited at a substrate temperature of 550°C was found to be crystallized. The Ce-doped film sputtered at 550°C has the cubic polycrystlline structure (randomly oriented) of $BaTiO_3$ (Fig. 1). Absence of the characteristic peaks of Ce-species in the diffraction pattern suggests the complete solubilization of Ce in $BaTiO_3$.

The surface morphology of the film was observed by SEM. The scanning electron micrograph in Fig. 2 show that the grains grown were homogeneous. Also, there are dropelets on the surface of film. The stoichiometric transfer from the target to film was analysed by EDAX. The chemical composition of the Ce-doped $BaTiO_3$ film was analysed in three different zones:

– on an aggregate (Table II);
– in an area between the aggregates (Table III);
– on the entire area showed in micrograph of Fig. 2 (Table IV).

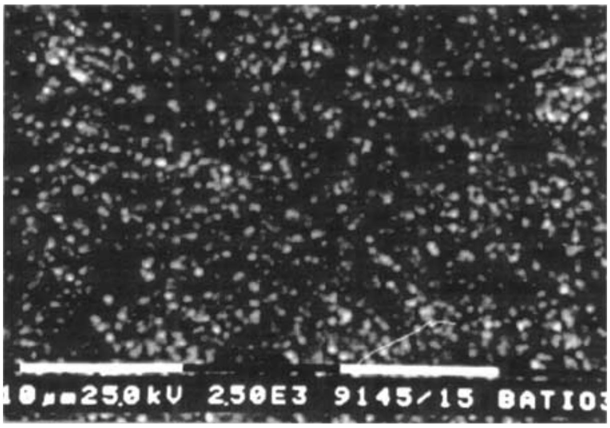

Figure 2 Scanning electron micrographs of $BaTiO_3$ doped with 5.5 mol%CeO_2 film.

TABLE II Composition of an agglomerate on the $BaTiO_3$ doped with 5.5 mol%CeO_2 film

	Composition, wt%	
Element	Element	Oxide
Ba	36.63	40.89
Ti	30.99	51.70
Ce	6.03	7.41
Total		100.00

TABLE III Composition in an area between the agglomerates on the $BaTiO_3$ with 5.5 mol%CeO_2 film

	Composition, wt%	
Element	Element	Oxide
Ba	36.20	40.42
Ti	31.26	52.14
Ce	6.06	7.4
Total		100.00

TABLE IV Composition on the entire area showed in Fig. 2

Element	Composition, wt% Element	Composition, wt% Oxide
Ba	38.10	42.54
Ti	31.08	51.85
Ce	4.57	5.61
Total		100.00

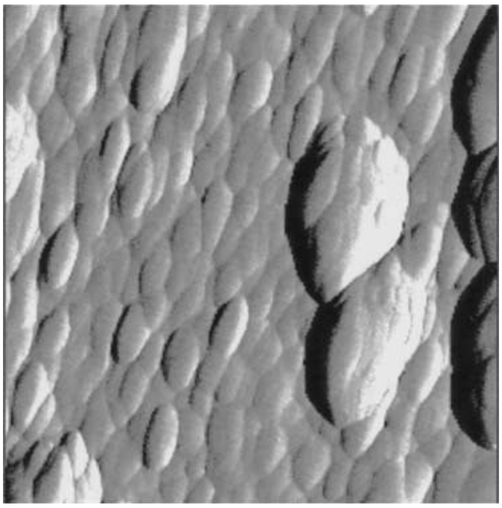

Figure 3 AFM pictures of $BaTiO_3$ doped with 5.5 mol%CeO_2 film sputtered on Si-Pt.

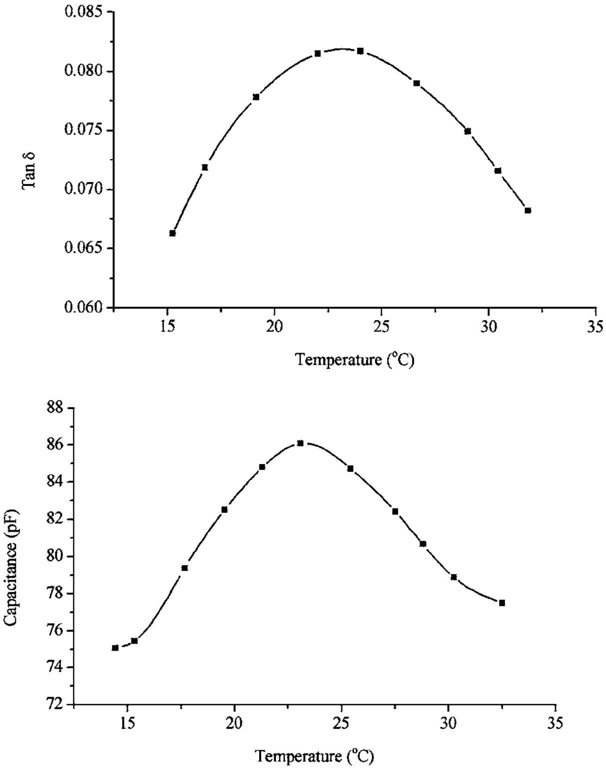

Figure 4 Capacitance and dielectric loss (tan δ) vs temperature of $BaTiO_3$ doped with 5.5 mol%CeO_2 film sputtered on Si-Pt.

Table I presents a CeO_2 concentration in the droplet as (7.41%), which is bigger than that of the target (5.5%). This rise on the CeO_2 concentration in the droplet is due to segregation of the dopant at grain boundaries and by the local inhomogeneity of the target composition. The composition on an aggregate and the composition between two droplets are approximately identical, in the analysed points. Though, the close value of the dopant concentration (5.61%) comparative with that of the target, was obtained for the entire area presented in the SEM micrograph (Fig. 2). That prove the same composition for both film and target.

The particulars of the film surface topography and the growth mechanism can be carried out using the AFM. Fig. 3 shows the surface of the Ce-doped BaTiO3 film deposited at 550°C. The average surface roughness over a scan area is 36.88 nm and 10.376 nm for the area without the aggregates. The top view of this film looks like a network with a grain size of 160 nm-width and 475 nm-height. On the other hand, we can see some grains measuring 0.675/1.105 μm, that increase in roughness. The aggregates rended from the target were deposited on the substrate as the large grains observed in Fig. 3. The grain sizes are in good agreement with previous results for the particle-size dependence. For particle sizes less than 120 nm, the symmetry at room temperature is cubic, while for larger particle sizes, the tetragonal, ferroelectric phase is found [13, 21].

The capacitance was measured as a function of temperature at 1 KHz to verify the existence of the ferroelectric-paraelectric phase transition. Fig. 4, shows the temperature characteristics of capacitance and dielectric loss for the Ce-doped $BaTiO_3$ film. A broad transition in the region of 23°C is seen. The maximum values of capacitance and dielectric loss at 23°C (Curie point) were 86 pF respectively, $\tan\delta = 0.0875$. The small grains size of the film contributes to peaks broadening. In general, the decrease and broadening of the dielectric peak, and the increase of the loss tangent in film may be attributed to the amaller grain size and lower packing density of the films compared to that of the bulk ceramics. Also, the lower value of the capacitance may be due to the existence of a non-ferroelectric surface layer at the film-electrode interface [22, 23].

4. Conclusions

Ferroelectric thin films of Ce-doped $BaTiO_3$ have been deposited by rf sputtering in 100%Ar, at a substrate temperature 550°C. The X-ray diffraction and EDAX studies indicate that the cubic films with perovskite-type structures are obtained on Si-Pt substrate. The broad peaks in the C-T and tan δ-T curves at Curie temperature confirm the ferroelectricity of the rf spputered $BaTiO_3$ doped with 5.5 mol%CeO_2 films. The decrease of the Curie temperature from 125°C (T_c of $BaTiO_3$ undoped) to 23°C (T_c of $BaTiO_3$-5.5 mol%CeO_2 film) and SEM-EDAX analysis confirm the deposition of the $BaTiO_3$-5.5 at.%Ce film with the target composition.

Acknowledgements

We would like to express our thanks to Mr. P. Budau from the NANOTECH.-Company for AFM analysis.

References

1. P. J. HARROP and D. S. CAMPBELL, *Thin Solid Films* **2** (1968) 273.
2. F. T. WOOTEN, *Proc. IEEE* **55** (1967) 564.

3. R. S. MULLER and J. CONRAGAN, *IEEE Trans. Electron. Devices* **ED-12** (1965) 590.
4. J. R. FIEBIGER and R. S. MULLER, *J. Appl. Phys.* **38** (1967) 1948.
5. A. B. KAUFMAN, *IEEE Trans. Electron. Devices* **ED-16** (1969) 562.
6. N. F. BORELLI and M. M. LAYTON, *ibid.* **ED-16** (1969) 511.
7. G. W. TAYLOR, *ibid.* **ED-16** (1969) 565.
8. K. FUJIMOTO, Y. KOBAYASHI and K. KUBOTA, *Thin Solid Films* **169** (1989) 249.
9. T. NAGAMOTO, T. KOSAKA, S. OMARI and O. OMOTO, *Ferroelectrics* **9** (1971) 91.
10. C. A. T. SALAMA and E. SICIUNAS, *J. Vac. Sci. Technol.* **9** (1971) 91.
11. O. X. JIA, Z. Q. SHI and W. A. ANDERSON, *Thin Solid Films* **209** (1992) 2230.
12. J. H. KIM and S. HISHITA, *J. Mater. Sci.* **30** (1995) 4645.
13. K. UCHINO, N. LEE, T. TOBA, N. USUKI, H. ABURATANI and Y. YTO, *J. Ceram. Soc. Jpn.* **100** (1992) 1091.
14. W. S. CLABAUGH, E. M. SWIGGARD and R. GILCHRIST, *J. Res. Natl. Bur. Std.* **56**(5) (1956) 289, RP 2677.
15. K. KUDAKA, K. ILZUMI and K. SASAKI, *Am. Ceram. Soc. Bull.* **61** (1982) 1236.
16. T.-T. FANG and H. B. LIN, *J. Amer. Ceram. Soc.* **72**(10) (1989) 1899.
17. T.-T. FANG, H. B. LIN and J. B. HWANG, *J. Mater. Sci. Lett.* **9** (1990) 688.
18. *Idem. J. Amer. Ceram. Soc.* **73**(11) (1990) 3363.
19. FU-SU YEN, CHEN T. CHANG and YEN-HWEI CHANG, *ibid.* **73**(11) (1990) 3422.
20. T. TUNKASIRI and G. RUJIJANAGUL, *J. Mater. Sci. Lett.* **13** (1994) 165.
21. K. UCHINO, E. SADANAGA and T. HIROSE, *J. Amer. Ceram. Soc.* **72** (1989) 1555.
22. Y. IJIMA, *Japan J. Appl. Phys.* **24** (1985) 401.
23. T. KAWANO, T. SEI and T. TSUCHIA, *J. Mater. Sci.* **31** (1991) 2178.

Received 24 April 2000
and accepted 1 May 2001